Application of Meshfree Method to Elastic-Plastic Fracture Mechanics Parameter Analysis

S. Hagihara[1], M. Tsunori[2], T. Ikeda[3] and N. Miyazaki[3]

Abstract: The element-free Galerkin (EFG) method is applied to the calculation of elastic-plastic fracture mechanics parameters such as the J-integral and T*-integral. The fields of displacement, strain and stress for a crack problem are obtained using the elastic-plastic EFG method. Then the elastic-plastic fracture mechanics parameters J-integral and T*-integral are calculated from path and domain integrals. In the finite element analysis, paths for the path integral and domains for the domain integral are selected depending on finite element mesh division. On the other hand, they can be arbitrarily selected in the EFG method, and we can use a simple integral path and domain such as a circular shape surrounding a crack tip, which can provide efficient numerical integral formulae for the path and domain integrals. In a crack growth problem, the simple integral path and domain can easily move together with the crack tip, as the crack tip advances. This paper presents a method for calculating the J-integral and T*-integral in a framework of the EFG method. The proposed method is applied to both a stationary crack problem and a stable crack growth problem. The results obtained from the EFG method are compared with those of the finite element method and experiments to show the effectiveness of the EFG method to the elastic-plastic fracture mechanics parameter analysis.

Keyword: meshfree method, element-free Galerkin method, fracture mechanics parameter, elasto-plastic, T*-integral.

[1] Saga University, Saga, Saga, JAPAN
[2] Ishikawajima-Harima Heavy Industries, Yokohama, Kanagawa, JAPAN
[3] Kyoto University, Kyoto, Kyoto, JAPAN

1 Introduction

It is necessary to calculate fracture mechanics parameters of a crack in evaluating the integrity of a cracked structure. When materials with high toughness are used as structural materials, ductile fracture is expected as a fracture mode. In such a case, elastic-plastic fracture mechanics parameters should be evaluated for the crack. The J-integral [Rice, J. R. (1968)] and T*-integral [Atluri, S. N., Nishioka, T. and Nakagaki, M. (1984)] are typical elastic-plastic fracture mechanics parameters.

In the case of stable crack growth, the J-integral loses path-independence, hence loses its physical meaning and the T*-integral should be used instead of the J-integral [Miyazaki, N. and Nakagaki, M. (1995)]. Integral forms of fracture mechanics parameters such as the J-integral and T*-integral can be calculated using the results of a finite element (FE) analysis. For a crack growth problem, it is necessary to move finite elements or to remesh a finite element model in the vicinity of a crack tip after crack propagation [Nishioka, T., Furutuka, J., Tchouikov, S. and Fujimoto, T. (2002)] [Fujimoto, T., Nishioka, T. (2006)] [Nishioka, T., Tchouikov, S., Fujimoto, T. (2006)]. In such a case, integral paths and domains are usually constrained by the FE division. That is, the integral paths are usually selected as passing through the integral points of finite elements or the nodes of finite elements, at which the stresses and strains are made smooth. It is also cumbersome to move the integral paths and integral domains together with the crack tip, because it is necessary to redefine the integral paths and domains by relating them with finite elements. Meshfree methods that are the element-free Galerkin (EFG) method [Be-

lytschko, T., Lu, Y. Y. and Gu, L. (1994)], the meshless local Petrov-Galerkin (MLPG) method [Atluri, S. N. and Zhu, T. (1998)], the smoothed particle hydrodynamics (SPH) method [Libersky, L. D., Petschek, A. G., Carney, T. C., Hipp, J. R. and Allahdadi, F. A. (1993)] and other methods are widely applied to many problems which are nonlinear, crack, large deformation and 3-dimensional problem [Chen, W. H. and Guo, X. M. (2001)] [Chen, W. H., Chen, C. H. (2005)] [Han, Z. D. and Atluri, S. N. (2004)] [Han, Z. D., Rajendran, A. M., Atluri, S. N. (2005)] [Gao, L., Liu, K., Liu, Y. (2006)] [Randles, P. W. and Libersky, L. D. (1996)]

The element-free Galerkin (EFG) method [Belytschko, T., Lu, Y. Y. and Gu, L. (1994)], one of meshfree methods, is a method alternative to the FE method. When the EFG method is used, the integral paths and domains for the calculation of elastic-plastic fracture mechanics parameters can be arbitrarily selected in the EFG method, and we can use a simple integral path and domain such as a circular shape surrounding the crack tip, which can provide efficient numerical integral formulae for path and domain integrals. In a crack growth problem, the simple integral paths and domains can easily move together with the crack tip, because they are free from finite elements. Several papers have published on the application of the EFG method to the calculation of the J-integral [Wu, C. D., He, P. X. and Li, Z. (2002)] [Rao, B. N. and Rahman, S. (2004)] [Kargarnovin, M. H., Toussi, H. E. and Fariborz, S. J. (2004)], but there has been no paper concerning the efficient computation of elastic-plastic fracture mechanics parameters that utilizes the features of the EFG method. This paper presents a method for calculating the J-integral and T*-integral in the framework of the EFG method. The proposed method is applied to both a stationary crack problem and a stable crack growth problem.

2   Method of analysis

2.1   Weak form of elastic-plastic element-free Galerkin method

A weak form of the EFG method for elastic-plastic problems is described in the following. Based on the hypothesis that the elastic strain $\boldsymbol{\varepsilon}^e$ and the plastic strain $\boldsymbol{\varepsilon}^p$ are independent each other, the total strain $\boldsymbol{\varepsilon}$ is written in separable form as follows:

$$\boldsymbol{\varepsilon} = \boldsymbol{\varepsilon}^e + \boldsymbol{\varepsilon}^p \tag{1}$$

The incremental form of strain is given as:

$$\Delta\boldsymbol{\varepsilon} = \Delta\boldsymbol{\varepsilon}^e + \Delta\boldsymbol{\varepsilon}^p \tag{2}$$

A weak form for the EFG method is given by the following equation including a penalty factor α in order to impose the essential boundary conditions.

$$
\begin{aligned}
&\int_V \delta\Delta\boldsymbol{\varepsilon}^T(\boldsymbol{\sigma}^{N-1} + \Delta\boldsymbol{\sigma})dV \\
&\quad - \int_S \delta\Delta\mathbf{u}^T(\overline{\mathbf{T}}^{N-1} + \Delta\overline{\mathbf{T}})dS \\
&\quad - \int_V \delta\Delta\mathbf{u}^T(\overline{\mathbf{F}}^{N-1} + \Delta\overline{\mathbf{F}})dV \\
&\quad + \int_{S_u} \alpha\delta\Delta\mathbf{u}^T(\mathbf{u} - \overline{\mathbf{u}})dS = 0
\end{aligned}
\tag{3}
$$

By using the nodal displacement vector, the following discrete form is derived.

$$
\begin{aligned}
&\int_V [\delta\Delta\mathbf{q}^T\mathbf{B}^T\boldsymbol{\sigma}^{N-1} + \delta\Delta\mathbf{q}^T\mathbf{B}^T(\mathbf{D}^e + \mathbf{D}^p)\mathbf{B}\Delta\mathbf{q}]dV \\
&\quad - \int_S \delta\Delta\mathbf{q}^T\mathbf{N}^T(\overline{\mathbf{T}}^{N-1} + \Delta\overline{\mathbf{T}})dS \\
&\quad - \int_V \delta\Delta\mathbf{q}^T\mathbf{N}^T(\overline{\mathbf{F}}^{N-1} + \Delta\overline{\mathbf{F}})dV \\
&\quad + \int_{S_u} \alpha\delta\Delta\mathbf{q}^T\mathbf{N}^T(\mathbf{u} - \overline{\mathbf{u}})dS = 0
\end{aligned}
\tag{4}
$$

where $\boldsymbol{\sigma}^{N-1}$, $\Delta\boldsymbol{\sigma}$, $\overline{\mathbf{T}}^{N-1}$, $\Delta\overline{\mathbf{T}}$, $\overline{\mathbf{F}}^{N-1}$, $\Delta\overline{\mathbf{F}}$ and $\Delta\mathbf{u}$ are stress, incremental stress, external traction, incremental external traction, body force, incremental body force and incremental displacement, respectively. δ denotes the variational operator. Superscript N-1 denotes the previous (N-1)th time step. $\mathbf{B}$, $\mathbf{D}^e$, $\mathbf{D}^p$ and $\mathbf{N}$ denote the strain-nodal displacement matrix, the elastic stress-strain matrix,

the plastic stress-strain matrix, the interpolation function matrix determined from the moving least square (MLS) method, respectively. The J_2 flow theory is used to make the plastic stress-strain matrix $\mathbf{D}^p$. Since $\delta\Delta\mathbf{q}$ is arbitrary virtual displacement, we obtain the incremental form of equilibrium equation of a total system in the following form:

$$\mathbf{K}\Delta\mathbf{q} = \Delta\mathbf{F}^a + \mathbf{F}^p + \mathbf{R} \tag{5}$$

where
$\mathbf{K}$ = elastic-plastic stiffness matrix including a term due to the penalty factor,
$\Delta\mathbf{q}$ = incremental nodal displacement vector,
$\Delta\mathbf{F}^a$ = incremental external force vector,
$\mathbf{D}^p$ = vector due to the penalty factor,
$\mathbf{R}$ = residual force vector

The incremental nodal displacements within each load increment are obtained by solving equation (5) for $\Delta\mathbf{q}$. The total nodal displacements are obtained by accumulating the incremental ones in each step. If the internal force is equilibrium with the external force, $\mathbf{R}$ becomes zero, otherwise the imbalance force is corrected in each increment by the Newton-Raphson scheme. Background cells are needed to perform integration over analyzed region. Triangles generated by using the Delaunay tessellation are used as background cells. Either the Lagrange multiplier method or the penalty function method is utilized for the treatment of the essential boundary conditions in the EFG method. We employ the penalty function method in the present analysis.

$\mathbf{B}$ and $\mathbf{N}$ in equation (4) are written by using a local shape function determined by the MLS method. The local shape function is made from the sampling nodes in the domain of influence. In the present EFG method, the linear basis function $\mathbf{p}(\mathbf{x})$ is used, and the approximate displacement function $u^h(\mathbf{x})$ can be written as follows:

$$\mathbf{p}(\mathbf{x})^T = [1, x, y] \tag{6}$$

$$u^h(\mathbf{x}) = \mathbf{p}(\mathbf{x})^T \mathbf{a}(\mathbf{x}) \tag{7}$$

$\mathbf{a}(\mathbf{x})$ is determined so as to minimize the following function.

$$J = \sum_{I}^{n} w(\mathbf{x} - \mathbf{x}_I)[\mathbf{p}(\mathbf{x})^T \mathbf{a}(\mathbf{x}) - u_I]^2 \tag{8}$$

The following exponential type of a weight function is employed in this analysis.

$$w_I(d_I) = \begin{cases} \dfrac{e^{-(d_I/C)} - e^{-(d_{mI}/C)^2}}{1 - e^{-(d_{mI}/C)^2}} & \text{if} \quad d_I \leq d_{mI} \\ 0 & \text{if} \quad d_I > d_{mI} \end{cases} \tag{9}$$

where $d_I = \|x - x_I\|$, $C = \beta \cdot d_{mI}$. β is a parameter which determines configuration of the weight function.

The trianglular background cells generated by the Delaunay tessellation are used to perform domain integration. The information of triangles is generated by the Delaunay tessellation using the initial node data of the EFG method. Searching nodes within a domain of influence to make the shape function of the MLS method consumes large amount of computational time. The shape functions of the MLS method are made from sampling nodes searched by the directed graph theory [Hagihara, S., Tsunori, M., Ikeda, T. and Miyazaki, N. (2003)]. The directed graph also uses the information of the triangles generated by the Delaunay tessellation. The searching nodes to make the shape function by directed graph theory can reduce the searching time for nodes.

2.2 Implementation of J-integral for EFG method

The path independent parameter J-integral proposed by Rice (1968) is well known to fracture mechanics problems. The mathematical representation for the J-integral on the contour as shown in Fig. 1 is given as follows:

$$J = \int_{\Gamma} [W n_1 - t_i u_{i,1}] d\Gamma \tag{10}$$

where W is the strain energy density defined by the following equation.

$$W = \int_0^{\varepsilon_{ij}} \sigma_{ij} d\varepsilon_{ij}$$

where σ_{ij}, ε_{ij} and u_i are the components of stress tensor, strain tensor and displacement vector, respectively. $(\ )_{,1}$ denotes $\partial(\ )/\partial X_1$. The summation convention is applied to the subscripts. Γ is

an arbitrary contour enclosing a crack tip counterclockwise in Fig. 1, $d\Gamma$ is an infinitesimal arclength along Γ, and t_i is the traction vector. Γ_ρ is a contour enclosing the vicinity of the crack-tip. n_1 is a component of X_1 direction of a normal vector **n** along Γ. Since strain, stress and
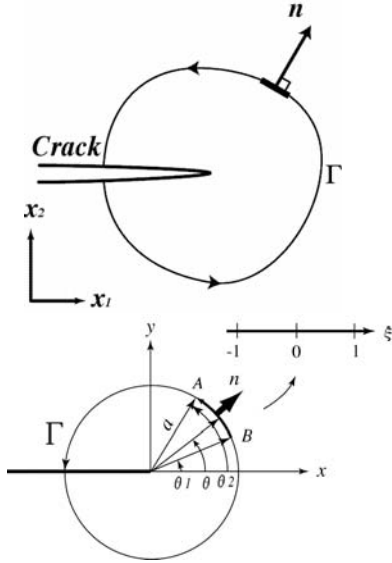

Figure 2: Circular integral path for J-integral and mapping of integral path to ξ-axis

displacement at an arbitrary point can be calculated by the MLS method, a line integral is implemented on an arbitrary circle independent of nodes and background cells. To perform the integration given by Eq. 10 along the circle we define the local ξ-coordinate along the circle as shown in Fig. 2. When the function is integrated along the arc from θ_1 to θ_2, the arbitrary point on the circle, the center of which is identical to the crack tip shown in Fig. 2, is represented as follows:

$$\begin{cases} x = a\cos\theta \\ y = a\sin\theta \end{cases} \qquad (11)$$

where a is the radius of the circle. θ is the angle as shown in Fig. 2. The J_n along Γ_c which is the arc of the circle from θ_1 to θ_2 is transformed to the following equation, using the local coordinate ξ.

$$J_n = \int_{\Gamma_c} [Wn_1 - t_i u_{i,1}] d\Gamma$$
$$= \int_{-1}^{1} \left[\left\{ W\cos\theta - \left(t_x \frac{\partial u_x}{\partial x} + t_y \frac{\partial u_y}{\partial x} \right) \right\} \frac{a(\theta_2 - \theta_1)}{2} \right] d\xi$$

(12)

where

$$\begin{cases} t_x &= \sigma_x(x,y)\cos\theta + \tau_{xy}(x,y)\sin\theta \\ t_y &= \sigma_y(x,y)\sin\theta + \tau_{xy}(x,y)\cos\theta \\ \theta &= \frac{1}{2}(\theta_1 + \theta_2) - \frac{1}{2}(\theta_1 - \theta_2)\xi \end{cases}$$

Each J_n transformed to the local coordinate is numerically calculated by the Gauss-Legendre quadrature. J is obtained from summation of all J_n as follows:

$$J = \sum J_n \qquad (13)$$

2.3 Implementation of T*-integral for EFG method

The path independent integral parameter T*-integral proposed by Atluri et al. [Atluri, S. N., Nishioka, T. and Nakagaki, M. (1984)] is used to detect the crack tip severity of a propagating crack. This parameter is useful to problems subjected to loading and unloading in elastic-plastic range such as a crack growth problem. The mathematical representation for the T*-integral is given as follows, for the domain shown in Fig.3:

$$T* = \int_{\Gamma_\rho} [Wn_1 - t_i u_{i,1}] d\Gamma$$
$$= \int_{\Gamma} [Wn_1 - t_i u_{i,1}] d\Gamma - \int_{V-V_\rho} [W_{,1}n_1 - \sigma_{ij}\varepsilon_{ij,1}] dV$$
$$= J_L - J_D$$

(14)
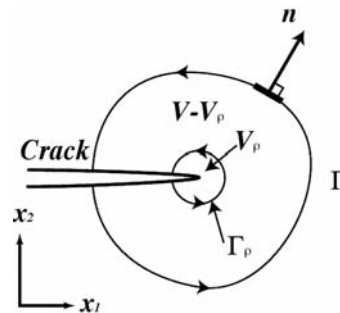
The T*-integral is separable to a line integral J_L

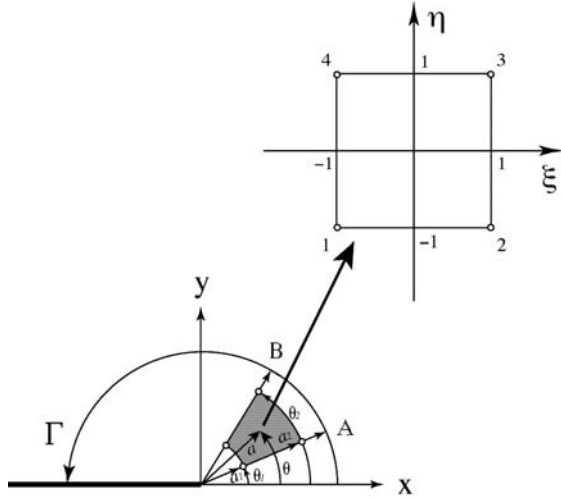Figure 3: Integral path and domain for T*-integral

Figure 4: Circular integral path and domain for T*-integral and mapping of integral domain to $\xi - \eta$ coordinate system

and a the *J*-integral, we can obtain it from the same procedure as shown in 2.2. Hereafter we will show how to calculate the domain integral J_D in detail. As shown in Fig.4, a subdomain is defined as the domain ranging from θ_1 to θ_2 and from a_1 to a_2. An arbitrary point in the subdomain defined by a and θ can be expressed by local coordinates (ξ, η) shown in Fig. 4, as follows:

$$\begin{cases} a & = & \frac{1}{2}(a_1 + a_2) - \frac{1}{2}(a_1 - a_2)\xi \\ \theta & = & \frac{1}{2}(\theta_1 + \theta_2) - \frac{1}{2}(\theta_1 - \theta_2)\eta \end{cases} \quad (15)$$

Then the J_D of the subdomain, J_{Dn}, can be obtained by performing the integration with respect to the local coordinates (ξ, η), as follows:

$$J_{Dn} = \iint f(x,y)dxdy \\ = \int_{-1}^{1}\int_{-1}^{1} f(a\cos\theta, a\sin\theta)\det[J]d\xi d\eta \quad (16)$$

$$[J] = \begin{bmatrix} \dfrac{dx}{d\xi} & \dfrac{dy}{d\xi} \\ \dfrac{dx}{d\eta} & \dfrac{dy}{d\eta} \end{bmatrix} \quad (17)$$

where $f(a\cos\theta, a\sin\theta)$ is an integrand in J_D expressed by the local coordinates. $\det|J|$ denotes the determinant of the Jacobian matrix $[J]$. The

J_{Dn} can be obtained numerically by the Gauss-Legendre quadrature, using the solution of the EFG method. Finally the T*-integral is obtained from summation of all J_{Ln} and J_{Dn} as follows:

$$T* = \sum (J_{Ln} - J_{Dn}) \quad (18)$$

Near a crack-tip area for the FE analysis, discontinuity between elements is conspicuous, i.e. the stresses and strains obtained from the analyses are usually unreliable within V_ρ. In order to circumvent such a problem, V_ρ is set to a finite value. in general [Brust, F. W., Nishioka, T., Atluri, S. N. and Nakagaki, M. (1985)]. We can obtain continuous displacements, strains, and stresses at the arbitrary point due to using the MLS method of EFG method, so that V_ρ can be set to zero and still reliable T*-integral is secured. Thus, the accurate and meaningful crack-tip state is evaluated. Since the stress and strain can be obtained at an arbitrary point, we can use an arbitrary circular path and quadrature point for calculation of both the J-integral and T*-integral. The circular paths and domains can be moved to any place together with a crack tip, as shown in Fig.5, when the crack tip advances. We can obtain these fracture mechanics parameter easily by using the EFG method.
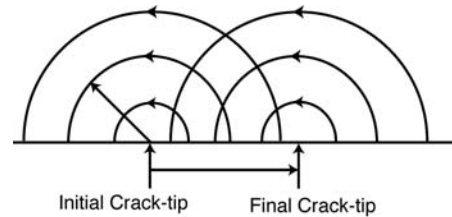

Figure 5: Circular integral path moving together with crack tip

3 Results and Discussion

3.1 *J-integral evaluation for stationary crack problem*

The fracture mechanics parameter J-integral is evaluated using line integration for a stationary crack problem of a center cracked plate under uniform tension. An elastic-plastic analysis is performed for the quarter model shown in Fig. 6,
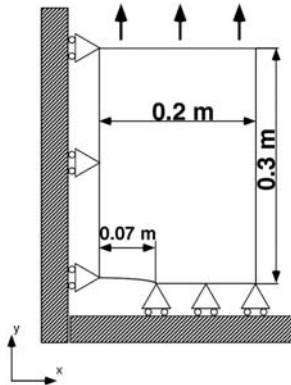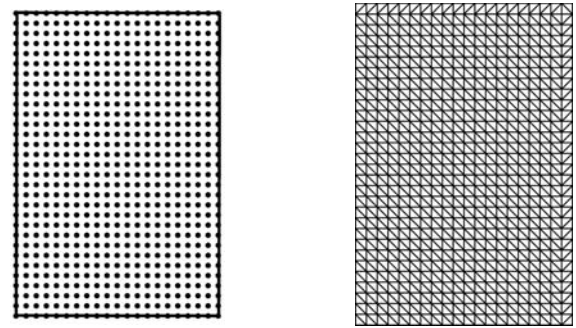
Figure 6: Quarter model of center cracked plate under tension

(a) Node configuration   (b) Triangular background cell

Figure 7: Node configuration and triangular background cells for EFG analysis (651-node model)

in which the dimensions and boundary conditions are depicted. A sample of the regular node configuration and triangular background cells are shown in Fig. 7. As mentioned in 2.1, the integral paths in the EFG method can be selected arbitrarily without constraint of finite elements. The circular paths surrounding the crack tip shown in Fig. 8 are used in the present analysis. Following are the material properties used in the present analysis:

$$E = 206 GPa, \quad v = 0.3, \quad \sigma_Y = 190 MPa,$$
$$H = 220 MPa$$

where E, v, σ_Y and H are Young's modulus, Poisson's ratio, yield stress and rate of strain hardening respectively. These material properties are corresponding to A533B Class 1 steel [Miyazaki, N.; Nakagaki, M. (1995)]. A bilinear approximation is employed for the stress-strain curve.

At first, the elastic J-integral values calculated from the EFG analysis are compared with a reference solution obtained from the conversion of the stress intensity factor given in the handbook [Murakami, Y. (1987)] into the energy release rate. The path dependence of the J-integral normalized by the reference solution is shown in Fig. 9 for three EFG models, 176-nodes model, 651-nodes model and 4941-nodes model. Although the 176-nodes model and 651-nodes model give erroneous J-values at the paths near the crack tip, they provide accurate J-values at the paths 3 through 6 far from the crack tip. On the other hand, the
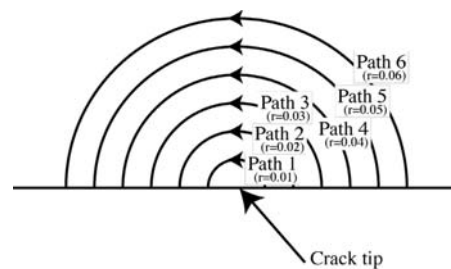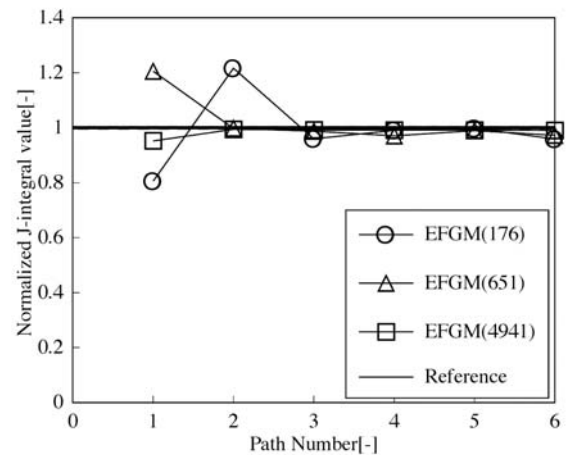

Figure 8: Integral paths for J-integra

Figure 9: Path depedence of elastic J-integral normalized by reference solution

4941-nodes model provides accurate results for all paths. The results of the elastic-plastic J-integral are compared between the EFG method and the FE method. Figure 10 shows the compar-
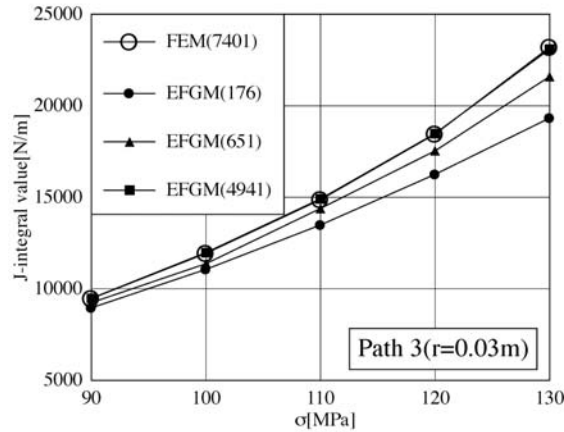
Figure 10: Comparison of Elastic-plastic J-integral among several EFG models and very fine FE model

Figure 11: Half model of CT specimen

ison among several EFG models and a very fine FE model. The FE solutions are obtained from the virtual crack extension method applied to a very fine regular mesh with 2400 eight-noded isoparametric elements and 7401 nodes. As the number of nodes increases in the EFG model, the results approach to those of the very fine FE model, and the 4941-nodes model of the EFG method gives almost the same results as the very fine FE model.

3.2 Evaluation of J-integral and T*-integral for stable crack growth

The J-integral and T*-integral are evaluated for stable crack growth in a compact tension (CT) specimen. Figure 11 shows a half model of the CT specimen used in the present analysis, in which the dimensions and boundary conditions are depicted. Figures 12 shows the node configuration and triangular background cells used in the analysis. The total number of nodes is 514. The nodes are concentrated in the vicinity of the crack tip.

A generation phase analysis for stable crack growth is performed to obtain the variations of the J-integral and T*-integral with crack growth. The EFG analysis is performed by controlling the displacement at a loading point and crack growth to trace the experimentally determined a half of displacement at the loading point versus crack growth curve shown in Fig. 13 [Miyazaki, N.
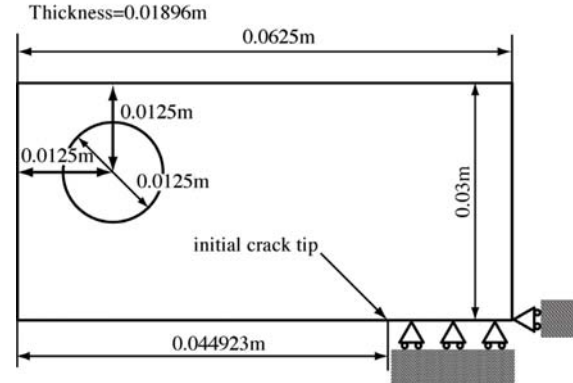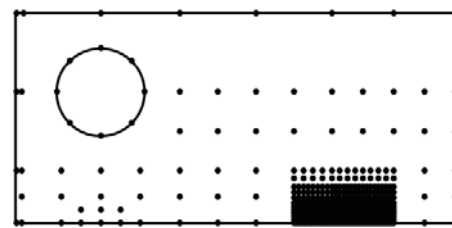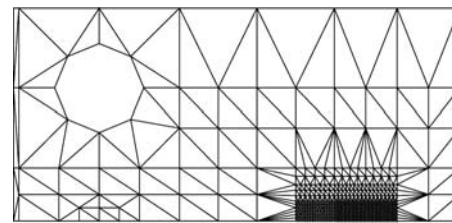

(a) Node configuration

(b) Triangular background cells

Figure 12: Node configuration and triangular background cells for EFG analysis

and Nakagaki, M. (1995)]. Such crack growth is simulated by releasing the constraint ahead of the crack tip. The circular paths shown in Fig. 14 are employed to calculate the J-integral. In addition to the path integral, the domain integral is required to calculate the T*-integral. Figure 15 shows an integral path and a mesh for domain integral for the T*-integral. The circular paths and the mesh shown in Figs 14 and 15 moves together with the crack tip, as the crack tip advances. The CT specimen is made of A533B Class 1 steel and the same material properties as in 3.1 are used in the present analysis. A bilinear approximation for
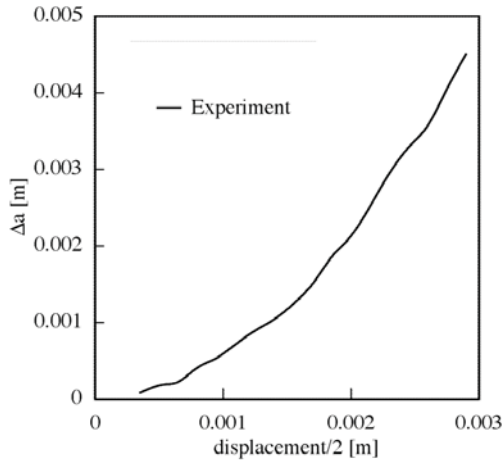
Figure 13: A half of displacement at loading point versus crack growth obtained from experiment
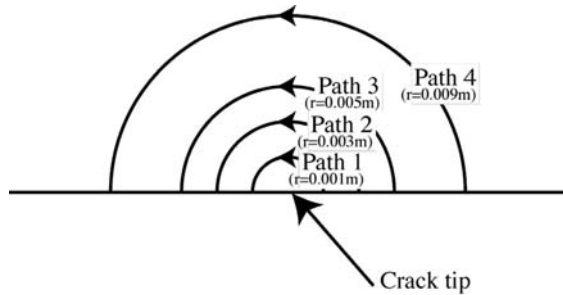

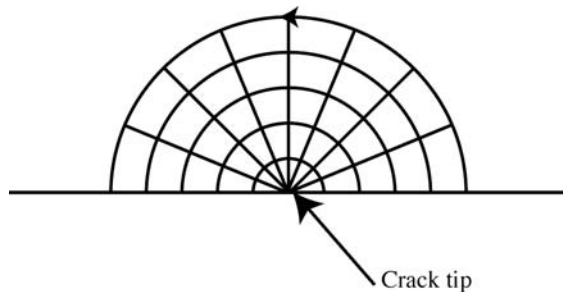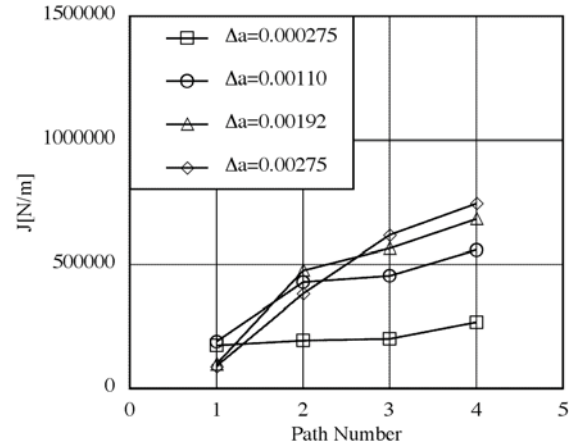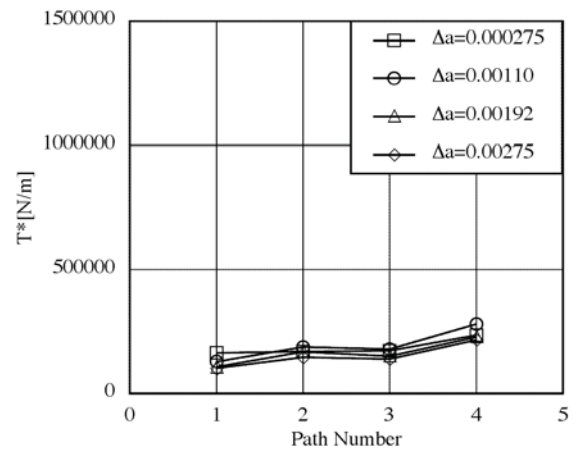Figure 14: Integral paths for J-integral

Figure 15: Integral path and mesh for domain integral for T*-integral

stress strain curve is also assumed in the present analysis.

Figures 16(a) and 16(b) show the path dependence of the elastic-plastic fracture mechanics parameters, J-integral and T*-integral. The J-integral

(a) J-integral

(b) T*-integral

Figure 16: Path dependence of elastic-plastic fracture mechanics parameters for stable crack growth

shows the path dependence after crack growth, which means that it does not represent the crack tip severity after crack growth. On the other hand, the T*-integral shows good path independence after crack growth. Thus it is valid fracture mechanics parameter representing the crack tip severity even after crack growth. Figure 17 shows a J-integral versus crack extension curve, that is, a J-resistance curve obtained form the EFG analysis, together with those evaluated from the simple formulae J_D(EXP) by Ernst [Ernst, H. A. (1981)] and J_{MC}(EXP) by Merkle and Corten [Merkle, J. G. and Corten, H. T. (1974)], using the experimen-
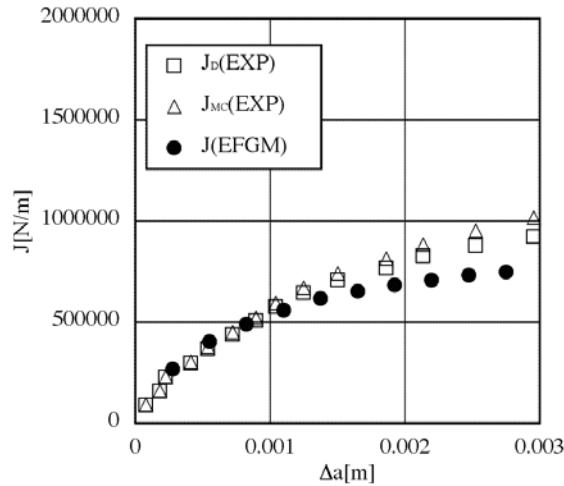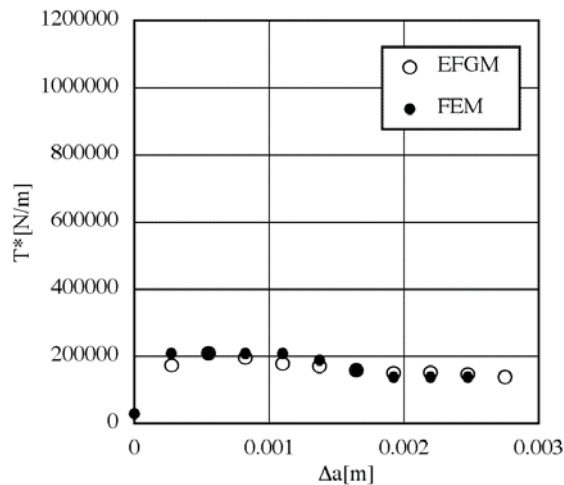
Figure 17: J-resistance curve

Figure 18: T*-resistance curve

creases with crack growth, and the latter keeps almost constant during stable crack growth. So such a constant T*-value can be used as a material property for stable crack growth, and we can perform the application phase analysis of stable crack growth and predict the behavior of stable crack growth in an arbitrary structure.

4   Conclusions

The EFG method is applied to both a stationary crack problem and a stable crack growth problem. The J-integral is evaluated in the former problem, and both J-integral and T*-integral are evaluated in the latter problem. The J-integral and T*-integral based on the results obtained from the EFG analysis are compared with those of the FE analysis and experimental results. Compared with the FE method, the EFG method provides reasonable accurate J-integral and T*-integral. In the finite element analysis, paths for the path integral and domains for the domain integral are selected depending on finite element mesh division. On the other hand, in the EFG method they can be arbitrarily selected and easily moved together with the advancing crack tip, and we can use a simple integral path and domain such as a circular shape surrounding a crack tip, which can provide efficient numerical integral formulae for the path and domain integrals. Due to such attractive features, the EFG method can be used as an analytical tool for elastic-plastic crack problems.

tally obtained displacement at the loading point. The T*-resistance curve obtained from the EFG analysis is shown in Fig. 18, together with that of the FEM analysis [Miyazaki, N. and Nakagaki, M. (1995)]. The J-resistance curve obtained from the EFG analysis agrees well with those of experimental results, and the T*-resistance curve obtained from the EFG analysis agrees well that of the FE analysis. It is therefore concluded that the EFG method can be used to evaluate the elastic-plastic fracture mechanics parameters for stable crack growth. In comparison of the J-resistance curve and the T*-resistance curve, the former in-

References

Atluri, S. N.; Nishioka, T.; Nakagaki, M. (1984): Engineering Fracture Mechanics, Incremental Path-Independent Integrals in Inelastic and Dynamic Fracture Mechanics, *Engineering Fracture Mechanics*, 20- 2, pp.209-244.

Atluri, S. N.; Zhu, T. (1998): Meshless local Petrov-Galerkin (MLPG) approach in computational mechanics, *Computational Mechanics*, Vol. 22, No. 2, pp.117-127.

Belytschko, T.; Lu, Y. Y.; Gu, L. (1994): Element-Free Galerkin Method, *International Journal for Numerical Methods in Engineering*., 37, pp.229-256.

Brust, F. W.; Nishioka, T.; Atluri, S. N.; Naka-gaki, M. (1985): Further studies on elastic-plastic stable fracture utilizing the T* integral, *Engineering Fracture Mechanics*, Vol. 22, No. 6, pp.1079-1103.

Chen, W. H.; Guo, X. M. (2001): Element Free Galerkin Method for Three-dimensional Structural Analysis, *CMES: Computer Modeling in Engineering & Sciences*, Vol.2, No.4, pp.497-508.

Chen, Wen-Hwa; Chen, Cheng-Hung (2005): On Three-Dimensional Fracture Mechanics Analysis by an Enriched Meshless Method, *CMES: Computer Modeling in Engineering & Sciences*, Vol. 8, No. 3, pp. 177-190.

Ernst, H. A. (1981): Estimation on J-integral and tearing modulus from a single specimen test record, *ASTM STP* 743, 476.

Fujimoto, T.; Nishioka, T. (2006): Numerical Simulation of Dynamic Elasto Visco-plastic Fracture Using Moving Finite Element Method, *CMES: Computer Modeling in Engineering & Sciences*, Vol. 11, No. 2, pp. 91-102.

Gao, L.; Liu, K.; Liu, Y. (2006), Applications of MLPG Method in Dynamic Fracture Problems: *CMES: Computer Modeling in Engineering & Sciences*, Vol. 12, No. 3, pp. 181-196.

Hagihara, S.; Tsunori, M.; Ikeda, T.; Miyazaki, N. (2003): Element-free Galerkin Method using Directed Graph and Its Application to Creep Problems, *Computational Mechanics*, 31, pp.489-495.

Han, Z. D.; Atluri, S. N. (2004): Meshless Local Petrov-Galerkin (MLPG) approaches for solving 3D Problems in elasto-statics, *CMES: Computer Modeling in Engineering & Sciences*, Vol.6, No.2, pp.169-188.

Han, Z. D.; Rajendran, A. M.; Atluri, S. N. (2005): Meshless Local Petrov-Galerkin (MLPG) Approaches for Solving Nonlinear Problems with Large Deformations and Rotations, *CMES: Computer Modeling in Engineering & Sciences*, Vol. 10, No. 1, pp. 1-12.

Kargarnovin, M. H.; Toussi, H. E.; Fariborz, S. J. (2004): Elasto-plastic element-free Galerkin method, *Computational Mechanics*, Vol.33, No.3, pp.206-214.

Libersky, L. D.; Petschek, A. G.; Carney, T. C.; Hipp, J. R.; Allahdadi, F. A. (1993): High strain lagrangian hydrodynamics –A three dimensional SPH code for dynamic material response, Journal of Computational Physics, 109, pp.67-75.

Merkle, J. G.; Corten, H. T. (1974): A J Integral Analysis for the Compact Specimen, Considering Axial Force as Well as Bending Effects, *Trans. ASME, Journal of Pressure Vessel Technology*, 96-4, pp.286-292.

Miyazaki, N.; Nakagaki, M. (1995): Two-dimensional finite element analysis of stably growing cracks in inhomogeneous materials, *International Journal of Pressure Vessels and Piping*, Vol.63, No.3, pp.249-260.

Murakami, Y. (1987): Stress Intensity Factors Handbook, Pergamon Press, Vol.1, pp.3-5.

Nishioka, T.; Furutuka, J.; Tchouikov, S.; Fujimoto, T. (2002): Generation-phase simulation of dynamic crack bifurcation phenomenon using moving finite element method based on delaunay automatic triangulation, *CMES: Computer Modeling in Engineering & Sciences*, Vol. 3, No.1, pp.129-145.

Nishioka, T.; Tchouikov, S.; Fujimoto, T. (2006): Numerical Investigation of the Multiple Dynamic Crack Branching Phenomena, *CMC: Computers, Materials & Continua*, Vol. 3, No. 3, pp. 147-154.

Randles, P. W.; Libersky, L. D. (1996): Smoothed particle hydrodynamics, *Couputer Methods in Applied Mechanics and Engineering*, 139, pp.375-408.

Rao, B. N.; Rahman, S. (2004): An enriched meshless method for non-linear fracture mechanics, *International Journal for Numerical Methods in Engineering*, Vol.59, No.2, pp.197-223.

Rice, J. R. (1968): A Path Independent Integral and the Approximate Analysis of Strain Concentration by Notches and Cracks , *Journal of Applied Mechanics* , 35, pp.379-386.

Wu, C. D.; He, P. X.; Li, Z. (2002): Extension of J integral to dynamic fracture of functional graded material and numerical analysis, *Computers & Structures*, Vol.80, No.5-6, pp.411-416.